

Current Topics

The Ni-Containing Carbon Monoxide Dehydrogenase Family: Light at the End of the Tunnel?[†]

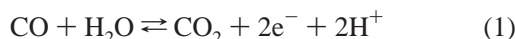
Paul A. Lindahl*

Departments of Chemistry and of Biochemistry and Biophysics, Texas A&M University, College Station, Texas 77843-3255

Received November 12, 2001; Revised Manuscript Received December 17, 2001

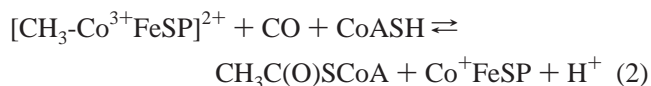
Metalloenzymes seem to “come of age” when their structures are known at atomic resolution, spectroscopic and catalytic properties are basically understood, and genetic expression systems are available. Such foundations allow detailed mechanistic and spectroscopic properties to be probed and correlated to structure. The objective of this paper is to summarize what is known about the title group of enzymes, and show that, to a large degree, they have come of age. I apologize to those involved in aspects that I do not cover, or do so inadequately. Previous reviews should be consulted for other perspectives and emphases (1–5).

Ni-containing carbon monoxide dehydrogenases are phylogenetically related, but they vary in terms of metabolic role, subunit composition, and catalytic activity. Monofunctional enzymes that exclusively catalyze the reversible oxidation of CO to CO₂ (reaction 1) are called carbon monoxide dehydrogenases (CODHs)¹ and are specified by a subscript indicating the host organism.

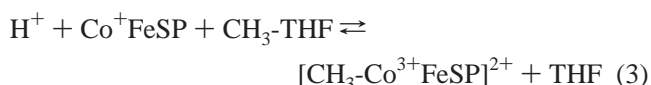


Bifunctional enzymes that additionally catalyze the synthesis

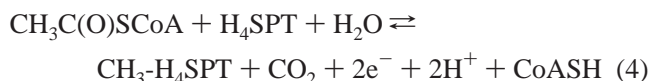
of acetyl-CoA (reaction 2) are called acetyl-CoA synthases/carbon monoxide dehydrogenases (ACS/CODHs).



CoFeSP in reaction 2 is the corrinoid–iron–sulfur protein, a heterodimer containing a cobalamin in one subunit and an Fe₄S₄ cluster in the other (1). Reduced Co⁺ cobalamin accepts a methyl group from CH₃-THF in reaction 3, catalyzed by methyltransferase (6).



Another group of bifunctional ACS/CODHs catalyze the decarbonylation of acetyl-CoA (reaction 4).



H₄SPT is tetrahydrosarcinapterin, an archaeal analogue of THF.

These enzymes are housed in evolutionarily primitive organisms many of which can grow exclusively on simple inorganic compounds (7). Wächtershäuser has implicated ACS/CODH-like reactions as participating in the origin of life (8). Organisms that were present prior to the appearance of O₂ may have used these enzymes as “tools” for extracting energy from environments that increasingly contained energy-rich organic molecules (7). Organisms housing these enzymes play critical roles in the global carbon cycle (9), antibiotic-

[†] This work was supported by the National Institutes of Health (Grant GM46441) and the Department of Energy (Grant DE-F603-01ER15177).

* To whom correspondence should be addressed. Phone: (979) 845-0956. Fax: (979) 845-4719. E-mail: Lindahl@mail.chem.tamu.edu.

¹ Abbreviations: CODH_{Gs}, monofunctional carbon monoxide dehydrogenases, with the superscript Gs indicating the genus and species of the organism from which the enzyme was isolated; ACS/CODH_{Gs}, bifunctional enzymes that catalyze the synthesis and/or degradation of acetyl-coenzyme A as well as the reversible reduction of CO₂ to CO; CoFeSP, corrinoid–iron–sulfur protein; THF, tetrahydrofolate; CoA, coenzyme A; EPR, electron paramagnetic resonance; XAS, X-ray absorption spectroscopy; ENDOR, electron nuclear double resonance.

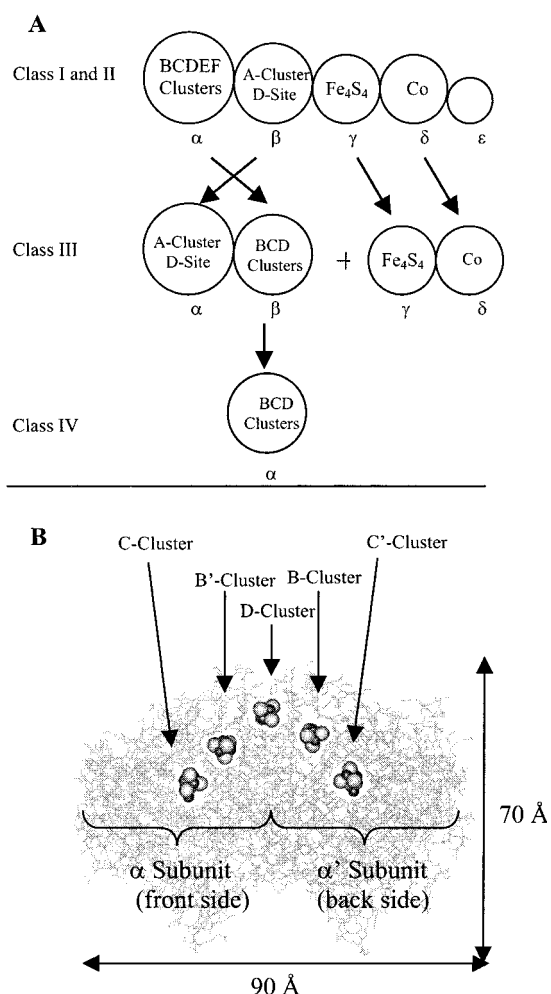


FIGURE 1: (A) Subunit relationships among the four classes of CODHs. The switch in α and β designations in class I/II vs class III enzymes arises because of relative molecular mass differences. Class I/II α sequences contain extra regions that house the putative E- and F-clusters, and are thus larger than the homologous class III/IV β subunits. Class I/II β sequences lack a 30 kDa N-terminus region present in class III α subunit homologues. Other details are given in the text. (B) Structure of homodimeric CODH_{Rr} (13). Protein residues that obscured the view of the metal-sulfur clusters are not shown. CODH_{Ch} has a similar overall structure (12).

associated colitis and nosocomial infections (10), and the degradation of environmental pollutants (11).

The Ni-containing CODH family of enzymes can be divided into four classes (7). Class I enzymes are ACS/CODHs found in obligate autotrophic methanogens such as *Methanobacterium thermoautotrophicum*, where they synthesize acetyl-CoA from CO₂/H₂. Class II enzymes are ACS/CODHs involved in acetoclastic methanogenesis. Both class I and II enzymes are composed of five different types of subunits (α , β , γ , δ , and ϵ) as illustrated in Figure 1A. Class III enzymes are ACS/CODHs found in homoacetogens, and consist of two autonomous proteins, including an $\alpha_2\beta_2$ tetramer (ACS/CODH) and a $\gamma\delta$ heterodimer (CoFeSP). Class III α , β , γ , and δ subunits are homologous to the β , α , γ , and δ subunits of the class I/II enzymes, respectively. The ϵ subunit of the class I/II enzymes has no class III homologue. Class IV enzymes are monofunctional α_2 homodimers where α is homologous to the α subunit of class I/II enzymes and to the β subunit of class III enzymes. Found in anaerobic CO-utilizing bacteria such as *Rhodospirillum*

rubrum and *Carboxydotherrmus hydrogenofomans*, these monofunctional enzymes catalyze CO/CO₂ redox but not the synthesis or degradation of acetyl-CoA.

X-ray Structure of the CODH from *C. hydrogenofomans* at 1.63 Å Resolution (12) and *R. rubrum* at 2.8 Å Resolution (13). The structures of these two proteins are basically equivalent. Both are ~130 kDa homodimers with a transverse twofold rotation axis (Figure 1B). Dimers contain five metal-sulfur clusters of three types, called B, C, and D. The Fe₄S₄ D-cluster bridges the subunits and is located near the surface of the protein along the rotation axis. Each subunit contains another Fe₄S₄ cluster, called the B-cluster, located ~10 Å away from D. Extending ~11 Å further along each D-B cluster axis is the C-cluster of the other subunit. Viewed from one orientation, the C-B'-D-B-C' cluster arrangement has an inverted V shape with the D-cluster at the apex and a C-cluster at the base of each leg.

The only significant difference between the two structures involves the C-cluster (Figure 2, middle structures). The CODH_{Ch} structure was determined to significantly higher resolution than CODH_{Rr}, and it seems reasonable to assume that differences arise from uncertainties of fitting the lower-resolution data. However, structural differences could also arise from differences in conditions used to crystallize the proteins, or from the protein structures themselves.

The Dobbek C-cluster (Figure 2, top structure) consists of one Ni, four Fe, and five sulfide ions. It is coordinated by five Cys residues (one to each metal ion) and one His residue to one of the irons [almost certainly ferrous component II or FCII; see below (14)]. The cluster can be divided into a [Ni-S-Fe] subsite (involving FCII) and an [Fe₃S₄] subsite. Three sulfides of the [Fe₃S₄] subsite constitute the *proximal face* and coordinate the metals of the [Ni-S-Fe] subsite. The *distal face*, composed of three irons and one μ^3 sulfide, points toward the B-cluster. The three proximal-face sulfides are also μ^3 (when linked to the [Ni-S-Fe] subsite), while the sulfide in the [Ni-S-Fe] subsite is μ^2 . Each iron is tetracoordinate and tetrahedral. Each Fe of the [Fe₃S₄] subsite has four S donors, while the Fe of the [Ni-S-Fe] subsite has three S donors and one N donor. The Ni is tetracoordinate with four S donors arranged in a square plane. The Ni is displaced 0.3 Å above this plane. The Drennan C-cluster (Figure 2, multicolored middle) is essentially a NiFe₃S₄ cubane bridged to FCII.

The C-cluster is buried 18 Å below the surface of the protein. Small molecules probably come and go through a tunnel that extends from the ends of the protein dimer to the Ni of each C-cluster. From the C-cluster, the tunnel continues toward the B-cluster at which point it diverges toward the protein surface, bypassing the D-cluster.

Conserved Amino Acid Residues. Eighteen sequences of class I, II, and IV α subunits and class III β subunits have been aligned (7), with selected regions shown in Table 1. Eight are from classes I and II, including those from archaea *M. thermoautotrophicum*, *Methanococcus jannaschii* (sequence 1), *Archaeoglobus fulgidus* (sequences 1 and 2), *Methanosarcina frisia* (sequences 1 and 2), *Methanosarcina thermophila*, and *Methanosaeta soehngenii*. Ten sequences are class III/IV-like, from bacteria *R. rubrum*, *Clostridium thermoaceticum* (also called *Moorella thermoacetica*), *C. hydrogenofomans*, *Clostridium difficile* (sequences 1 and 2), *Clostridium acetobutylicum* (sequences 1 and 2) and from

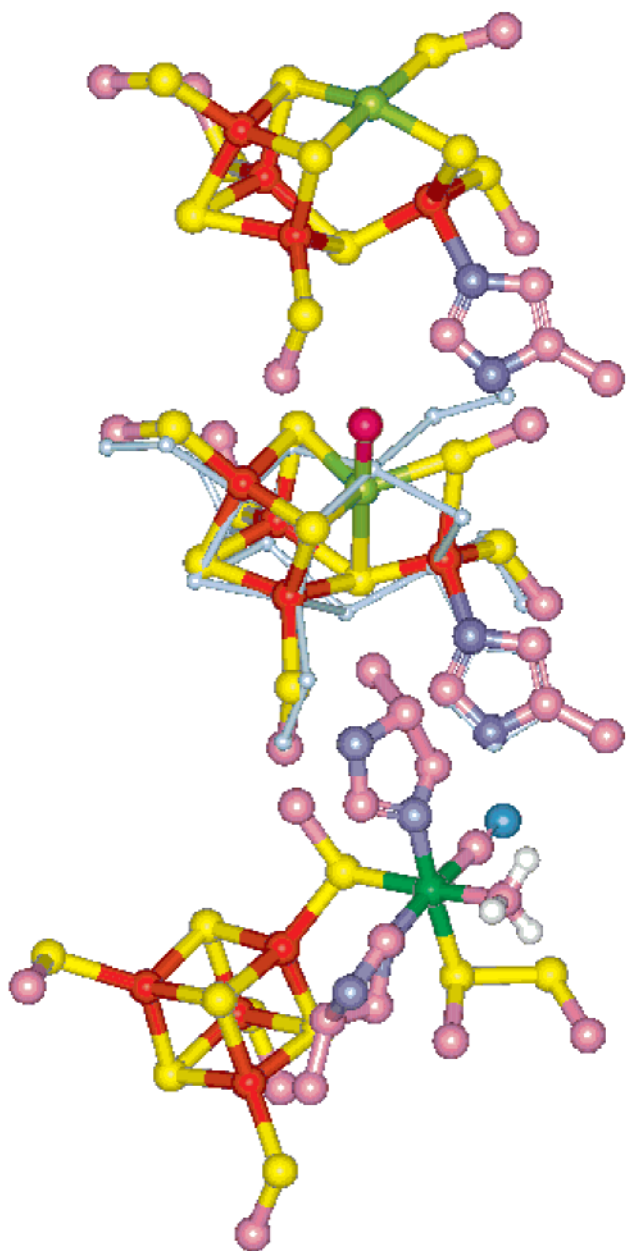


FIGURE 2: Structures of the Ni–Fe–S clusters in CODHs. (Top) The Dobbek C-cluster (12): Ni, green; Fe, rust-colored; S, yellow; N, purple; and C, pink. (Middle) The Drennen C-cluster (multi-colored) (13) with the Dobbek C-cluster (light blue) superimposed. The similarities between the two structures are remarkable. The only significant difference is the sulfur ion(s) that bridge the Ni and FCII and an extra unidentified ligand to the Ni (assumed to be CO). The color code is the same as that described above, with the unidentified ligand in red. (Bottom) The proposed structure of the A-cluster, shown with the methyl group and CO coordinated. The structure includes an Fe₄S₄ cubane bridged through a Cys sulfur to a Ni center. Other ligands to the Ni include two His nitrogens and a sulfur ion from the D-site cystine (shown here in the D_{ox} state). The color code is the same as that described above, but also blue for O and white for H.

archaea *A. fulgidus* (sequence 3), *M. jannaschii* (sequence 2), and *Methanopyrus kandleri*. Since the physiological function of the archaeon-housed “bacterial” enzymes is unknown, they are called “class III/IV-like”.

Cys ligands to the B-cluster are conserved throughout all sequences, but those to the D-cluster are not. Five D-ligating patterns can be discerned (Table 1). Conserved residues

(Table 2) are numbered differently for each protein, and to avoid confusion, we use the universal numbering scheme (7) in both tables. The arrangement characteristic of CODH_{Ch} and CODH_{Rr}, in which Cys070 and Cys078 are D-cluster ligands, is also present in sequences from *C. thermoaceticum*, *C. difficile*, and *C. acetobutylicum* (sequence 2). The second pattern, in which Cys075 probably substitutes for Cys070, is found in all class I/II sequences except for those from *M. soehngenii* and *A. fulgidus* (sequence 2). The pattern found in these two species lacks any Cys residues that could bind a D-cluster. The fourth pattern, evident in *C. acetobutylicum* sequence 1 and in *A. fulgidus* sequence 3, may coordinate the D-cluster using Cys070 and Cys073. The fifth pattern, evident in the class III/IV-like sequences from *M. kandleri* and *M. jannaschii* (sequence 2), has only one appropriate ligand for D-cluster coordination (Cys070). Thus, *D-cluster coordination appears to be highly variable, raising the possibility that this cluster is missing or altered in some enzymes.*

C-Cluster ligands are completely conserved except for those from *C. acetobutylicum* and *A. fulgidus* (sequence 2) which have Glu rather than Cys at position 335; in all other sequences, Cys335 is a ligand to FCII. Except for these differences, *all of these enzymes appear to contain C-clusters of uniform structure.* The majority of sequences exhibit a conserved His pattern involving positions 124, 127, 130, and 134 (or thereabout). His124 neighbors the [Ni–S–Fe] subsite of the C-cluster, while the other His residues are part of the tunnel (13), and could serve as a proton transfer relay. In some class III/IV-like sequences, this pattern has changed (Table 1). Class I/II enzymes contain two additional regions, absent in class III/IV-like sequences (positions 485–495 and 526–536), that almost certainly support Fe₄S₄ clusters dubbed E- and F-clusters. These putative clusters might reroute electron transfer along different paths (7). Lys725 is conserved in all but four class III/IV-like sequences, and has been proposed to stabilize the M–COO[−] species by H-bonding (13). Other interesting residues are highlighted in Table 1.

In summary, CODH sequences can be divided into class I/II and class III/IV-like groups, and these can be further divided into two and four subdivisions, respectively. Some organisms contain multiple CODH-encoding genes, but in all cases, they arise from different subdivisions. This suggests that *enzymes from different subdivisions play distinct metabolic roles*; i.e., the presence of two CODHs in an organism does not reflect simple redundancy.

Redox and Spectroscopic Properties of B- and D-Clusters. Most spectroscopic properties of the B- and C-clusters have been determined using ACS/CODH_{Ch} and CODH_{Rr}, though qualitatively similar features of other homologues, including CODH_{Ch} (15), suggest that these properties are universal. Prior to the crystal structure results being available, these enzymes had been known to contain B- and C-clusters but not the D-cluster. Crystal structure results confirmed that the C-cluster consists of a Ni ion associated with an Fe–S cluster that contained four irons, with one of these irons (FCII) unique and coordinated with His (14, 16). However, in contrast to the crystal structure, the spectroscopic model had the Ni ion bridged to an Fe₄S₄ cluster (14, 16, 17). How can the spectral properties of the enzyme now be reconciled with the structure?

Table 1: Sequence Alignment of the Subunit Containing B-, C-, and D-Clusters^a

ORGANISM	CLASS	RESIDUE NUMBER (UNIVERSAL)	070-----087	123-----137	228	251	297	333
<i>M. thermoautotrophicum</i>	I	FYAPFCDMCC...LCTYGKC	AHAGHARHLVDHLIE	SACH MD...D	IGHN	ICC		
<i>M. jannaschii I</i>	I	FYMPICDLCC...LCTFGKC	CHAGHSRHLVHHLIE	SAAH ID...D	IGHN	ICC		
<i>A. fulgidus I</i>	I or II	FYAPACDMCC...LCTMGKC	AHTGHARHML...HDIE	DAVH LD...S	IGHH	ICC		
<i>M. frisia I</i>	I or II	VVTPMCDQCC...YCTYGPC	CHAAHGRHLLDHLIE	ATVH LD...H	IGHN	LCC		
<i>M. frisia II</i>	II or I	VVTPMCDQCC...YCTYGPC	CHAAHGRHLLDHLIE	ATVH LD...H	IGHN	LCC		
<i>M. thermophila</i>	II	VITPMCDQCC...YCTYGPC	CHAAHGRHLLDHLIE	ATVH LD...H	IGHN	LCC		
<i>M. soehngenii</i>	II	MYSPADDT...CTLCTYGPC	AHTAHGRHLY...HWCL	AACH ID...S	YGHN	VCC		
<i>A. fulgidus II</i>	II or I	FYAPMQDF...CNLCTMGPC	AHTAHARHLVDHLIE	HSTH AD...H	VGHN	LCC		
<i>R. rubrum</i>	IV	CGFGSAGLCCRICLKGPC	AHSEHGRHIALAMQH	SRTH AD...L	NGHN	ICC		
<i>C. thermoaceticum</i>	III	CKIGYEGICCRFCMAGPC	AHCEHGNHIAHALVE	NQAH AD...Y	HGHN	ICC		
<i>C. hydrogenoformans</i>	IV	CGFGETGLCCRHCLQGPC	GHS GHAKHLAHTLKK	HRTS AD...L	HGHN	ICC		
<i>C. difficile I</i>	III or IV	CGFGQLQGVCCRICGMDPC	AHSDHARDIAHTL...A	HSTH ADGW	HGHE	MCC		
<i>C. acetobutylicum I</i>	III or IV	CKFKLEGLSCQLCSNGPC	TYSHHAYEAYRTLKA	ASCL AT...I	NGHQ	SIE		
<i>A. fulgidus III</i>	III or IV	CPFCEKGLSCQLCSMGPC	AYTYHAIEAAKTLKA	SSAM AT...C	NGHE	FIE		
<i>C. acetobutylicum II</i>	III or IV	CKFGKDGVCCKLCLANGPC	CYVHVVEVETARNLKA	VKTS STGL	TGHQ	CTC		
<i>C. difficile II</i>	III or IV	CGFGQLQGVCCRLCSNGPC	CYLHVVENTAKNLKN	VKSS STGL	TGHQ	CTC		
<i>M. jannaschii II</i>	III/IV?	CPYGLKGVYCIILCANGPC	CYVHCAENAAARALLS	TKTS HAGF	TGHQ	ATC		
<i>M. kandleri</i>	III/IV?	CPYKGQGVWCNICSNGPC	CYVHCLENAARALKS	VKTS ITG...	TGHQ	ATC		

ORGANISM	CLASS	RESIDUE NUMBER (UNIVERSAL)	485-----495	526-----536	671-----680	724	731	741
<i>M. thermoautotrophicum</i>	I	CTDCGWQCQRVC	CYTCGRCEQEC	NMGSCVSNNAH	QKA	TGV	VLGPH	
<i>M. jannaschii I</i>	I	CTECGWCNRNC	CYGCGRCEAIC	NCGSCLSNCH	QKA	TGV	ILGPH	
<i>A. fulgidus I</i>	I or II	CTQCGNCTIAC	CIACGRCEQVC	QIGSCVANAH	QKA	TGF	VVGPH	
<i>M. frisia I</i>	I or II	CADCGACYLAC	CIGCRRCEQVC	NIGSCVSNNAH	QKA	TGC	VLGAH	
<i>M. frisia II</i>	II or I	CADCGACLIAC	CIGCRRCEQVC	NIGSCVSNNAH	QKA	TGC	VLGPH	
<i>M. thermophila</i>	II	CADCGSCLYLV	CIGCRRCEQVC	NIGSCVSNNAH	QKA	TGC	VLGPH	
<i>M. soehngenii</i>	II	CTECNQCAFVC	CVGCQRCEQTC	NIGSCVANAH	QKA	TGV	VVQPS	
<i>A. fulgidus II</i>	II or I	CTQCMNCVFETC	CLACMKCEQAC	NTGSCVANS	HKA	TGF	VVGPH	
<i>R. rubrum</i>	IV	HMGSCVDNSR	EKA	SWA	HVGSV	
<i>C. thermoaceticum</i>	III	HMGSCVDNSR	GKA	TWW	HVGTM	
<i>C. hydrogenoformans</i>	IV	HMGSCVHNSR	EKA	TWA	HIGVF	
<i>C. difficile I</i>	III or IV	HMGSCVDISR	EKA	CYV	YLGIM	
<i>C. acetobutylicum I</i>	III or IV	SFGTCTDTGR	QKA	IFA	HLSPV	
<i>A. fulgidus III</i>	III or IV	SFGTCTDTGR	QKA	VFA	HVSPV	
<i>C. acetobutylicum II</i>	III or IV	NFGPCLAIGR	EQA	AFG	HLAIS	
<i>C. difficile II</i>	III or IV	NFGPCLAIGR	EQA	AFG	HLALP	
<i>M. jannaschii II</i>	III/IV?	NFGACLSIAR	EQA	TYA	HVSPV	
<i>M. kandleri</i>	III/IV?	HYGPCLAIGK	EQA	SSA	HVSPV	

^a Lines separate sequences into six patterns.

Let's start with the EPR and Mössbauer studies contributed by the Münck, Ragsdale, Ludden, and Lindahl groups (14, 18, 19). Under oxidizing conditions ($E \sim 50$ mV vs NHE), the B- and C-clusters are in their diamagnetic oxidized states, B_{ox} and C_{ox} , respectively. As potentials are lowered, these clusters are reduced to the B_{red} and C_{red1} states, respectively (20, 21). B_{red} exhibits an EPR signal ($g_{av} = 1.94$) typical of $[Fe_4S_4]^+$ clusters with $S = 1/2$ system spin states (18, 20). Mössbauer components associated with such clusters correspond to ~ 1.5 Fe_4S_4 clusters/monomer. The extra 0.5 cluster/monomer was previously unexplained, but may reflect the D-cluster. However, further studies are required to verify this.

Precursor C-Cluster. When grown on Ni-depleted nutrients under a CO atmosphere, the enzyme from *R. rubrum* ($CODH_{Rr}^*$) is catalytically inactive and devoid of Ni (22). Full activity develops after reducing $CODH_{Rr}^*$ and incubating it with $NiCl_2$. $CODH_{Rr}^*$ must therefore contain a Ni-deficient form of the C-cluster (called C^*) that can be converted to the native C-cluster. Mössbauer studies show that C^* is either an $[Fe_4S_4]^{2+/1+}$ cluster or a novel structure that has EPR, Mössbauer, and UV-vis features typical of such clusters. In the former case, activation would appear to involve a major structural rearrangement as Ni is inserted and a sulfide ion is sequestered from the environment.

Roberts and Ludden have studied the *coo* operon responsible for $CODH_{Rr}$ extensively, and have identified the *cooCTJ*

genes responsible for inserting the Ni into C^* (23). The $CooC$ homodimer binds and hydrolyzes ATP/GTP and inserts the Ni (24). $CooJ$ contains a His-rich C-terminus that binds up to four Ni ions (25). $CooT$ may be involved in metal ion discrimination (23). It is tempting to conclude that these proteins cause the major structural rearrangement suggested above, but recall that reduced $CODH_{Rr}^*$ can be activated in vitro by simply adding $NiCl_2$.

Redox and Spectroscopic Properties of the C-Cluster. At potentials below -200 mV, diamagnetic C_{ox} is reduced by one electron to the $S = 1/2$ C_{red1} state exhibiting an EPR signal with a g_{av} of 1.82 (18, 26). Mossbauer spectra reveal that C_{red1} contains four irons, two of which are called FCII and FCIII (the other two irons could not be individually characterized). FCIII is a high-spin Fe^{2+} that, along with the uncharacterized irons, probably constitutes the $[Fe_3S_4]$ subsite. FCII is a high-spin five- or six-coordinate Fe^{2+} , and is almost certainly the Fe of the $[Ni-S-Fe]$ subsite. ENDOR studies in the Hoffman lab indicate that a histidine residue ligates FCII (16). CN^- is a potent tight-binding inhibitor of CO/ CO_2 redox catalysis that binds to FCII in the C_{red1} state and displaces a strongly coupled OH^- group (14, 16, 27).

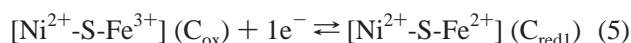
Since the late 1980s, Ni was assumed to be associated with the C-cluster, but evidence for this was inconclusive. Adding Ni to $CODH_{Rr}^*$ perturbed the electronic spin state of C_{red}^* and converted one of the irons of this precursor cluster into FCII (14). Hyperfine interactions between the

Table 2: Selected Residues in CODH_{Ch} and CODH_{Rr}^a

residue	CODH _{Ch}	CODH _{Rr}	universal	description
Cys	039	041	070	ligand to D-cluster
Cys	047	049	078	ligand to D-cluster
Cys	048	050	079	ligand to B-cluster
Cys	051	052	082	ligand to B-cluster
Cys	056	058	087	ligand to B-cluster
Cys	070	072	101	ligand to B-cluster
His	093	095	124	His pattern (H-bonded to Lys725?)
His	096	098	127	His pattern
His	099	101	130	His pattern
His	102	108	133/134	His pattern
His	195	202	231	conserved in class I/II, some class III/IV
Asp	219	223	252	(H-bonding network)
His	261	265	299	ligand to FCII of C-cluster
Cys	294	299	334	conserved in class I/II, some class III/IV
Cys	295	300	335	ligand to FCII of C-cluster
Cys	333	338	387	ligand to [Fe ₃ S ₄] of C-cluster
Cys	—	—	485	ligand to E-cluster (conjecture)
Cys	—	—	488	ligand to E-cluster (conjecture)
Cys	—	—	491	ligand to E-cluster (conjecture)
Cys	—	—	495	ligand to E-cluster (conjecture)
Cys	—	—	526	ligand to F-cluster (conjecture)
Cys	—	—	529	ligand to F-cluster (conjecture)
Cys	—	—	532	ligand to F-cluster (conjecture)
Cys	—	—	536	ligand to F-cluster (conjecture)
Leu	442	447	590	restriction in tunnel (not conserved)
Cys	446	451	594	ligand to [Fe ₃ S ₄] of C-cluster
Cys	476	481	625	ligand to [Fe ₃ S ₄] of C-cluster
Cys	526	531	675	ligand to Ni of C-cluster
His	—	—	680	conserved in class I/II
Lys	563	568	725	H-bonded to μ^2 -S of C-cluster?
His	579	584	741	conserved in most class III/IV
His	—	—	745	conserved in most class I/II

^a Universal numbers (7) and a description of the residues are included.

spin of C_{red1} and ⁶¹Ni were reported (28), but could not be confirmed (14). L-Edge XAS by Cramer and co-workers indicated a low-spin diamagnetic Ni²⁺ ion (29), a result supported by the square-planar geometry of the Dobbek structure. This diamagnetic Ni would not be part of the spin coupling mechanism, explaining the insignificant ⁶¹Ni hyperfine interactions. This result, along with the absence of FCII in C_{ox} Mössbauer spectra, suggests that the reduction of C_{ox} to C_{red1} corresponds to reaction 5.



To be compatible with the observed $S = 0$ and $S = 1/2$ spin states for C_{ox} and C_{red1}, respectively, the [Fe₃S₄] subsite should have a -1 core oxidation state (i.e., [Fe₃S₄][−]) for both C_{ox} and C_{red1}.

The coordination environment of the Ni in CODH_{Rr} was investigated by K-edge XAS (17). A Ni–Fe interaction at 2.8 Å was observed for a well-characterized [NiFe₃S₄] cubane model compound but not for the enzyme. The Ni in CODH_{Rr} was concluded not to be incorporated into a cubane, but possibly bridged to an Fe–S cluster and coordinated by two or three N/O and two S ligands. Near-edge studies suggested either tetrahedral or distorted geometry but not square-planar. These results and conclusions are not easily reconciled with the crystal structures. The Dobbek C-cluster seems less rigid than a cubane and thus less likely to exhibit strong Ni–Fe

interactions, but the observed all-sulfur square-planar environment is difficult to reconcile with the Ni site proposed from the XAS study.

The C-cluster exhibits two additional redox states called C_{red2} and C_{int} (18, 20, 30, 31). C_{red2} is in an $S = 1/2$ spin state and exhibits an EPR signal similar to that of C_{red1} but with a g_{av} of 1.86 (for ACS/CODH_{Ch}). The C_{red1}-to-C_{red2} conversion is redox-dependent and occurs (under an Ar atmosphere) in accordance with an E° of -520 mV. Numerous low-potential reductants, including CO and dithionite, can effect this reduction. Spectroscopic characteristics of C_{red2} have been difficult to study because B-clusters (and probably D-clusters) are paramagnetic under conditions where C_{red2} is present (14). It is clear, however, that FCII is present in C_{red2} spectra, and that the strongly coupled OH[−] evident in ENDOR studies of C_{red1} is absent (14, 16).

Heterogeneity. Spin intensities of all well-characterized EPR signals in ACS/CODH_{Ch}, including those from B_{red}, C_{red1}, and C_{red2} (and A_{red}-CO; see below), quantify to approximately 0.7, 0.3, 0.3, and 0.3 spin/ $\alpha\beta$, respectively (18–20). These intensities are below unity because samples are heterogeneous in terms of redox and spin states (20). My impression is that the problem occurs independently of laboratory and organism, though this is uncertain. Ludden and co-workers report that heterogeneity can be “cured” by preincubation with CO (32). Meyer’s group reports ~ 1.1 spins/monomer for C-cluster signals in CODH_{Ch} (15). Heterogeneity does not appear to arise from the process in which metal centers are built or installed into the protein. We recently cloned the genes encoding ACS/CODH_{Ch}, and expressed them in *Escherichia coli* (33). *E. coli* does not naturally contain enzymes in the CODH family, and thus presumably lacks the specific accessory proteins used by *C. thermoacetica* in metal-center assembly and insertion. However, the resulting recombinant protein was catalytically active and exhibited EPR signals with the same low-spin intensities as the native enzyme. This suggests that heterogeneity arises from factors *inherent* to the enzyme. Might the presence of a single D-cluster per dimer be involved?

Mechanism of CO/CO₂ Redox Catalysis. The most popular mechanism of CO oxidation (12–14, 16, 34) has CO binding to the Ni of the C-cluster and H₂O binding to FCII (Figure 3, top mechanism). This lowers the pK_a of the H₂O, yielding a nucleophilic OH[−] that attacks the Ni-bound CO. Ni binding to CO increases the electrophilicity of the carbonyl carbon and may induce dissociation of the OH[−] (16). A base accepts a proton from the resulting Ni-bound carboxylic acid group, encouraging CO₂ to dissociate as two electrons are delivered to the enzyme. Electrons exit the enzyme one at a time through the {B-cluster:D-cluster} “wire” (12, 13) as protons exit through the histidine relay pathway.

Many details of this mechanism require further testing before it can be considered established. Among the most contentious is the site to which two electrons are delivered as CO₂ dissociates, as well as the redox and spin state of this site. One possibility is that C_{red2} is two electrons more reduced than C_{red1}, and that C_{red1} accepts the electrons (21, 27, 35) (reaction 6).



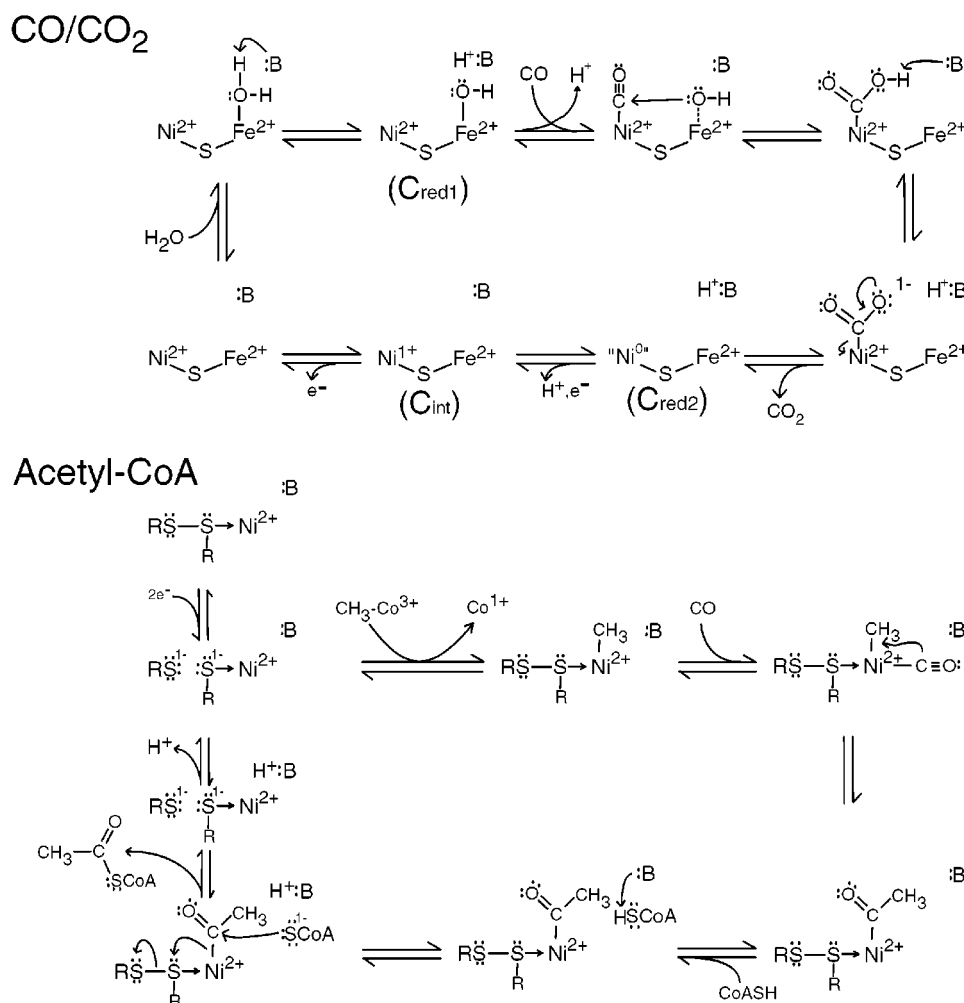


FIGURE 3: Proposed catalytic mechanisms for the oxidation of CO and reduction of CO₂, and for the synthesis of acetyl-CoA. See the text for details.

Both states are $S = 1/2$ states and thus may differ by two electrons, as required for this process. Moreover, E° for the C_{red1} -to- C_{red2} transition (-0.52 V) is near that for the CO₂/CO couple (-0.512 V). If electrons exit the enzyme one at a time, this proposal implies that the C-cluster should be stable in a redox state one electron more reduced than C_{red1} and one electron more oxidized than C_{red2} . Evidence for such a state, called C_{int} , has been obtained (31). One problem with this possibility is the lack of an obvious site on the C-cluster to deposit those two electrons. The electronic state of C_{red2} is very similar to that of C_{red1} . A two-electron reduction of C_{red1} , forming a state involving Ni⁺ and an all-ferrous [Fe₃S₄]²⁻ subsite, would yield an electronic state substantially different from C_{red1} . An electronic state involving Ni⁰ and [Fe₃S₄]⁻ would be similar to that of C_{red1} (as both d¹⁰ Ni⁰ and low-spin d⁸ Ni²⁺ would be diamagnetic), but there is no precedence for sulfide ions and thiolate groups supporting Ni⁰. Could an electronically delocalized trithiolato ligand like the [Fe₃S₄]⁻ subsite stabilize Ni⁰?

Ludden and co-workers have suggested a rather speculative mechanism that assumes spin coupling in nearly all C-cluster states (32, 36). The model was proposed before the crystal structure was reported, and it assumed some unrealized structural features (namely, that the C-cluster consisted of an [Fe₄S₄]⁺ cluster spin-coupled to a Ni-Fe binuclear center). In a "poststructure" publication, they retain the

fundamentals of their model by viewing the unrealized Ni-Fe center as the [Ni-Fe] subsite and the unrealized [Fe₄S₄]⁺ cluster as the [FeS_c] subsite (37). According to their model, C_{red2B} is an $S = 1/2$ state with an [Fe²⁺Ni²⁺] subsite, C_{red1} is an $S = 1$ state that is one electron more reduced than C_{red2B} and has an [Fe³⁺Ni²⁺-H⁻] subsite, C_{unc} is an $S = 1/2$ state that is one electron more reduced than C_{red1} and has an [Fe²⁺Ni²⁺-H⁻] subsite, and C_{red2A} is isoelectronic with C_{unc} but has the [FeS_c] subsite coupled to B_{red}. CO₂ reacts with C_{unc} , forming CO and C_{red2B} as products. Thus, C_{red2B} , C_{red1} , and C_{unc} ($\equiv C_{red2A}$) of the Ludden model are equivalent in terms of redox state to C_{red1} , C_{int} , and C_{red2} , respectively, in the "standard" mechanism. Characterizing C_{red1} as an even-spin state with Fe³⁺ in the [Ni-Fe] subsite is contrary to Mössbauer spectra of this state, and the order in which C-cluster EPR signals are proposed to develop and decay, according to the Ludden model, seems contrary to what is observed.²

Site-directed mutagenesis has been used to correlate C-cluster structure and function. Spangler et al. prepared a mutant CODH_{Rr} in which Val replaces His299, an FCII ligand (26). H299V is 1000 times less active than native CODH_{Rr}; it contains substoichiometric amounts of Ni and does not exhibit the C_{red1}/C_{red2} EPR signals. These results demonstrate the importance of this ligand in catalysis and redox, and suggest a link between FCII and the ability of

the cluster to coordinate Ni. A mutant was also prepared in which Ala replaced Cys675, a ligand to the Ni (36). The Ni content of C675A was similar to that of native CODH_R; however, the mutant was inactive, and its Fe–S clusters were not reduced when C675A was exposed to CO. Also, EPR signals from the C_{red1}/C_{red2} states were replaced by a new signal with a g_{av} of 2.16. Thus, C675 appear to be required for catalysis and redox, but not binding the Ni to the cluster. This is counterintuitive, given that Cys675 coordinates the Ni.

CO₂ Effects. CO₂ alters many properties of the metal centers (30). Incubating ACS/CODH_{Ct} in CO₂ increases the E° for the C_{red1}/C_{red2} conversion, the E° for the B_{ox}/B_{red} transition, and the E° for the A_{ox}/A_{red} transition. CO₂ perturbs the C_{red1} and B_{red} EPR signals, and it may convert ACS/CODH_{Ct} into a form in which clusters are reduced by a cooperative process. In the presence of a low-potential reductant like dithionite, CO₂ increases the rates at which C_{red1} converts to C_{red2} and that at which CN[−] dissociates from FCII. It “cures” batches of defective enzyme that had been unable to reduce their C-clusters from the C_{red1} to C_{red2} states (35). CO₂ increases the strength of CO binding to the A-cluster (introduced below) by ~10-fold, and inhibits the CO/acetyl-CoA exchange activity of ACS/CODH_{Ct}. The binding of CO₂ appears to cause a significant conformational change that reconfigures the metal centers in the enzyme such that redox potentials are matched and reductions occur rapidly and synchronously. Pre-steady state kinetic evidence indicates that ACS/CODH_{Ct} is activated for acetyl-CoA synthesis by CO₂ binding and a reduction of two to four electrons (39).

The Ludden group reported that CODH_R is activated for CO/CO₂ redox catalysis by CO binding and a one-electron reduction of a site having an E° of approximately −340 mV (37, 40, 41). In conflict with the standard model, they conclude that C_{red1} is not used in catalysis, as this state develops with an E° of −110 mV in CODH_R and is present at potentials at which the enzyme could not reduce CO₂. They suggest that C_{unc} binds and reduces CO₂. An important test of this would be to determine the E° for the C_{red1}-to-C_{red2} conversion in CODH_R.

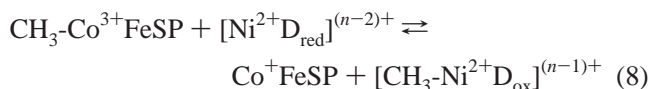
Redox and Spectroscopic Properties of the A-Cluster. Enzymes that catalyze the synthesis or decarbonylation of acetyl-CoA contain another type of metal center called the A-cluster, which serves as the active site for these reactions. It is located in the α subunit of class III-like enzymes and the β subunit of class I/II enzymes (42–44). The A-cluster is stable in either of two oxidation states, including an $S = 0$ state called A_{ox} and an $S = 1/2$ state called A_{red}-CO. Converting A_{ox} to A_{red}-CO involves one-electron reduction and CO binding. A_{red}-CO exhibits the NiFeC EPR signal,

so named because incorporating ⁶¹Ni ($I = 3/2$), ⁵⁷Fe ($I = 1/2$), and ¹³CO ($I = 1/2$) in this cluster hyperfine-broadens the signal. The elegant studies by Ragsdale, Wood, and Ljungdahl that demonstrated this provided the first evidence for a NiFe center in biology (1, 45).

The basic structure of this cluster was determined using EPR, ENDOR, Mössbauer, model compound synthesis, and XAS (1, 19, 45–47), with the strongest evidence being that obtained once methods were developed to isolate α subunits from ACS/CODH_{Ct} (42, 43). This procedure allowed the spectroscopic properties of the A-cluster to be examined without interference from clusters in the β subunit. Isolated α subunits contain four irons/ α and exhibit EPR and UV–vis properties typical of [Fe₄S₄]^{2+/1+} clusters. Treatment with aqueous Ni²⁺ yields a state that mimics the EPR, Mössbauer, CO binding, and redox properties of A_{red}-CO, suggesting that the A-cluster consists of a Ni ion spin-coupled to an Fe₄S₄ cluster. Mössbauer and UV–vis spectroscopies were used to determine that the Ni ion is reduced from the +2 to the +1 state in the reduction of A_{ox} to A_{red}-CO; thus, A_{ox} corresponds to [Fe₄S₄]²⁺–X–Ni²⁺, and A_{red}-CO corresponds to [Fe₄S₄]²⁺–X–Ni⁺–CO (42, 43).

The intensity of the NiFeC signal corresponds to only ~0.3 spin/ α , again significantly lower than the expected value of unity. The Ni of the A-cluster is labile and can be removed by 1,10-phenanthroline (48). This eliminates acetyl-CoA synthase activity and the ability to generate the A_{red}-CO state and the NiFeC signal. Reinsertion of Ni reactivates the enzyme and restores its ability to generate this state and signal. The amount of Ni removed and replaced (~0.3 Ni/ $\alpha\beta$) suggests that only ~30% of the A-clusters have labile Ni ions, are catalytically active, and can exhibit the NiFeC EPR signal (42, 48). The remainder have nonlabile Ni ions, do not exhibit the NiFeC signal, and are inactive.

Methylation of ACS_{Ct}. A methylated form of ACS_{Ct} can be prepared by treating the *reduced* enzyme with CH₃-Co³⁺FeSP (1, 49). The A-cluster is almost certainly the site to which the methyl group binds, but the species that must be reduced before methyl transfer occurs remains uncertain. This species was initially assumed to be the A-cluster itself, but Barondeau and Lindahl found that reductants unable to reduce A_{ox} can effect methylation (49). Other known redox sites on the enzyme were also eliminated, suggesting that ACS/CODH_{Ct} contains an unidentified $n = 2$ redox site which they called the D-site (not related to the D-cluster). They proposed that D was a redox-active disulfide, and designated activation and methyl group transfer from CH₃-Co³⁺FeSP to be reactions 7 and 8.



The methyl group transfers as a CH₃⁺ cation and most likely involves an S_N2 nucleophilic displacement (1, 50), and is unusual because it involves metal ions as both the methyl group donor and acceptor. D is a surrogate redox agent that allows the Ni to remain in the +2 state upon methylation. The {Ni²⁺D_{red}} unit is comparable to Co⁺ cobalamin in terms of nucleophilicity and can be viewed as the functional equivalent of “Ni⁰”.

² Low-temperature zero-field Mössbauer spectra of C_{red1} exhibit magnetic hyperfine interactions indicating a half-integer spin state, and high-temperature spectra exhibit the FCII doublet, with parameters of a ferrous ion. Four redox titrations of ACS/CODH_{Ct} have been reported, all qualitatively similar (18, 20, 21, 30). Although EPR-monitored titrations of CODH_R have not been reported, its redox behavior appears to be similar (14). As potentials are lowered from ~0 mV, the C_{red1} EPR signal appears first, followed by B_{red} and then C_{red2} as C_{red1} declines (depending somewhat on the presence or absence of CO₂). Similar properties were also observed in pre-steady state kinetic studies (21, 38). In contrast, the Ludden model seems to imply that in such titrations, C_{red2B} should appear first, followed by C_{red1}, C_{unc}, and finally C_{red2A}.

Proposed Structure of the A-Cluster. The proposed structure for the Ni-labile form of the A-cluster is shown (Figure 2, bottom) with the methyl group and CO bound, and with a Cys bridging ligand. In the A_{ox} state, the Ni is tetracoordinate with S_2N_2 donors and two cis open coordination sites. This arrangement is suggested because in organometallic complexes, CO inserts into metal–methyl bonds in which the methyl is bound on the same metal cis to the CO. It also rationalizes why 1,10-phenanthroline can remove Ni from this cluster. The nonbridging coordinated Cys sulfur forms a disulfide bond with another Cys, and this constitutes D_{ox} . Sequence alignment reveals that six Cys, three His, one Met, and numerous Asp/Glu residues are conserved (7). Three of these Cys residues probably coordinate the Fe_4S_4 portion of the A-cluster; one might bridge the cluster and Ni, and two might constitute the D-site. The Met and two His residues could also coordinate the Ni, while the remaining His could be used as a base for deprotonating CoA (51). The Ni of the A-cluster and the Co of the CoFeSP are probably at the surface of their respective proteins, as the methyl group probably transfers directly from one metal to the other.

Proposed Catalytic Mechanism of Acetyl-CoA Synthesis. We favor the following mechanism (43, 49, 51) (Figure 3, bottom mechanism). The D-site is reduced by two electrons, $CH_3-Co^{3+}FeSP$ binds ACS/CODH_{Ct}, and a methyl cation transfers to Ni^{2+} as D is oxidized. Then CO binds to the Ni^{2+} and inserts into the CH_3-Ni^{2+} bond, forming a $CH_3C(O)-Ni^{2+}$ group. A base abstracts the thiol proton of CoA, and the resulting thiolate attacks the carbonyl of the acetyl- Ni^{2+} group. Finally, D_{ox} is re-reduced as acetyl-CoA leaves. CO insertion and reductive elimination steps are common to organometallic chemistry, but are rare in biology. This mechanism has been embellished through the years but is derived from the seminal study of Wood and Ragsdale (52). Holm's well-characterized reaction sequence using Ni model complexes (46) was also critically important in developing this model. Whether substrates react in the proposed order has not been established. However, CoA probably reacts last, since the species with which it reacts (acetyl- Ni^{2+}) is formed from the reaction of the other two substrates. Other mechanisms employ the $A_{red}-CO$ state as a catalytic intermediate (1), but there is evidence that this state inhibits catalysis (49, 53). Further studies are required to resolve this.

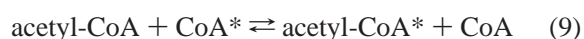
Tunnel Connecting the C- and A-Clusters, and $A \rightarrow C$ Coupling. Maynard and Lindahl discovered that as long as ACS/CODH_{Ct} is reduced, CO_2 can be used as a substrate in the synthesis of acetyl-CoA (53). In this case, CO is generated at the C-cluster by the reduction of CO_2 and it travels to the A-cluster where it is used in acetyl-CoA synthesis. Catalysis is unaffected when hemoglobin is included in assays as a CO "sponge", suggesting that the CO generated at the C-cluster migrates to the A-cluster through a proteinaceous tunnel. A complementary study subsequently confirmed the presence of the tunnel (54). Similar tunnels are found in other bifunctional enzymes in which the product of one reaction is the substrate of the other.

The effects of changing CO/ CO_2 concentrations on steady state acetyl-CoA rates show that CO activates ACS/CODH_{Ct} at low concentrations ($\sim 10 \mu M$), is a substrate at intermediate concentrations ($K_M \sim 300 \mu M$), and is an inhibitor at high concentrations ($K_I \sim 50-900 \mu M$) (55). Substrates CO and CO_2 compete for the C-cluster, while inhibitor CO molecules

bind cooperatively to a form of the enzyme that differs from that to which substrate CO and CO_2 bind. Substrate CO may migrate to the A-cluster from the C-cluster via the tunnel, while the inhibitor CO may bind directly to the A-cluster (and form $A_{red}-CO$) without going through the tunnel.

This raises the issue of whether the two active sites are coordinated in terms of kinetics and mechanism. k_{cat} and K_M for CO_2 reduction are 37 min^{-1} and 7 mM, respectively, while during synthesis of acetyl-CoA (with CH_3-Co^+FeSP and CoA included), the equivalent parameters are 200 min^{-1} and $380 \mu M$, respectively (39). Thus, the apparent second-order rate constant for CO_2 consumption increases ~ 100 -fold when ACS/CODH_{Ct} converts from reductase to synthase "mode"! Binding of the synthase substrates CoFeSP and CoA triggers this effect, and the conversion occurs with a k_{app} of $\sim 80 \text{ min}^{-1}$. Triggering, communication of information, and alteration of kinetic parameters are collectively termed $A \rightarrow C$ coupling. By monitoring CO production (using hemoglobin as a CO detector), Maynard and Lindahl found that $A \rightarrow C$ coupling precludes the release of CO from the enzyme (39). Coupling reroutes CO that is produced at the C-cluster through the tunnel and to the A-cluster, synchronizing the rates of the two activities. An ordered mechanism could synchronize events occurring at the two distant active sites. Thus, ACS/CODH_{Ct} operating in synthase mode using CO_2 as a substrate may be viewed as having a single active site composed of a cobalamin–A-cluster–tunnel–C-cluster unit.

Class I/II ACS/CODH Enzymes. The functions of class I/II subunits are now understood (56–58). The acetyl group of acetyl-CoA transfers to the Ni on the A-cluster of the β subunit. CO is eliminated and migrates to the α subunit where it is oxidized to CO_2 . The $\gamma\delta$ subunits transfer the methyl group to H_4SPT via an CH_3-Co^{3+} cobalamin intermediate. Grahame developed an assay catalyzed by the ACS/CODH of *Methanosarcina barkeri* in which 3'-dephospho-CoA (CoA^*) exchanges with CoA in acetyl-CoA (56).



The enzyme is reductively activated ($E^\circ = -486 \text{ mV}$, pH 6.5) in a step involving H^+ transfer (possibly corresponding to the reduction of the D-site). Reaction 9 occurred by a ping-pong mechanism, indicating the presence of an acetyl-enzyme intermediate. This high-energy intermediate has a ΔG° for hydrolysis of -9.5 kcal/mol .

Future Directions. The complexity and functional unity of the metal center structures, tunnels, and catalytic mechanisms employed by the CODH family of enzymes is impressive. Compared to what was known 20 years ago, the advances made have been significant, and we seem justified in proclaiming that these enzymes have come of age. On the other hand, compared to what is known about the best-understood enzymes, we can only see a faint light at the end of a long tunnel. Atomic level structures of acetogenic and methanogenic systems are required to advance our structural understanding of these enzymes, while further kinetic, spectroscopic, and redox studies are required to improve our understanding of their catalytic mechanisms. One fascinating aspect of these enzymes is their use of nickel. What special properties of Ni provide a selective advantage to organisms that use it? We have a partial answer—Ni (in

conjunction with Fe and S) allows organometallic type reactions to occur in biological systems—but a more complete answer requires further studies. Another important issue is what to do with this knowledge once we have it. Could uncovered principles of catalysis help synthesize new catalysts with useful properties? Might it be possible to genetically alter these enzymes to degrade toxic compounds? I am hopeful such applications will follow as that light at the end of the tunnel shines brighter.

ACKNOWLEDGMENT

I sincerely thank all of my students and postdocs that have researched these enzymes in my laboratory, for both their work and friendship.

REFERENCES

- Ragsdale, S. W., and Kumar, M. (1996) *Chem. Rev.* 96, 2515–2539.
- Ferry, J. G. (1995) *Annu. Rev. Microbiol.* 49, 305–333.
- Wood, H. G., and Ljungdahl, L. G. (1991) in *Variation in Autotrophic Life* (Shively, J. M., and Barton, L. L., Eds.) pp 201–250, Academic Press, New York.
- Fontecilla-Camps, J. C., and Ragsdale, S. W. (1999) *Adv. Inorg. Chem.* 47, 283–333.
- Ermiler, U., Grabarse, W., Shima, S., Goubeaud, M., and Thauer, R. K. (1998) *Curr. Opin. Struct. Biol.* 8, 749–758.
- Seravalli, J., Zhao, S. Y., and Ragsdale, S. W. (1999) *Biochemistry* 38, 5728–5735.
- Lindahl, P. A., and Chang, B. (2001) *Origins Life Evol. Biosphere* 31, 403–434.
- Huber, C., and Wächtershäuser, G. (1997) *Science* 276, 245–247.
- Bartholomew, G. W., and Alexander, M. (1979) *Appl. Environ. Microbiol.* 37, 932–937.
- Taege, A. J., and Adal, K. A. (1999) *Cleveland Clin. J. Med.* 66, 503–507.
- Huang, S., Lindahl, P. A., Wang, C., Bennett, G. N., Rudolf, F. B., and Hughes, J. B. (2000) *Appl. Environ. Microbiol.* 66, 1474–1478.
- Dobbek, H., Svetlitchnyi, V., Gremer, L., Huber, R., and Meyer, O. (2001) *Science* 293, 1281–1285.
- Drennan, C. L., Heo, J., Sintchak, M. D., Schreiter, E., and Ludden, P. W. (2001) *Proc. Natl. Acad. Sci. U.S.A.* 98, 11973–11978.
- Hu, Z., Spangler, N. J., Anderson, M. E., Xia, J. Q., Ludden, P. W., Lindahl, P. A., and Münck, E. (1996) *J. Am. Chem. Soc.* 118, 830–845.
- Svetlitchnyi, V., Peschel, C., Acker, G., and Meyer, O. (2001) *J. Bacteriol.* 183, 5134–5144.
- DeRose, V. J., Anderson, M. E., Lindahl, P. A., and Hoffman, B. M. (1998) *J. Am. Chem. Soc.* 120, 8767–8776.
- Tan, G. O., Ensign, S. A., Ciurli, S., Scott, M. J., Hedman, B., Holm, R. H., Ludden, P. W., Korszun, Z. R., Stephens, P. J., and Hodgson, K. O. (1992) *Proc. Natl. Acad. Sci. U.S.A.* 89, 4427–4431.
- Lindahl, P. A., Münck, E., and Ragsdale, S. W. (1990) *J. Biol. Chem.* 265, 3873–3879.
- Lindahl, P. A., Ragsdale, S. W., and Münck, E. (1990) *J. Biol. Chem.* 265, 3880–3888.
- Fraser, D. M., and Lindahl, P. A. (1999) *Biochemistry* 38, 15697–15705.
- Saravalli, J., Kumar, M., Lu, W.-P., and Ragsdale, S. W. (1997) *Biochemistry* 36, 11241–11251.
- Ensign, S. A., Campbell, M. J., and Ludden, P. W. (1990) *Biochemistry* 29, 2162–2168.
- Kerby, R. L., Ludden, P. W., and Roberts, G. P. (1997) *J. Bacteriol.* 179, 2259–2266.
- Jeon, W. B., Cheng, J., and Ludden, P. W. (2001) *J. Biol. Chem.* 276, 38602–38609.
- Watt, R. K., and Ludden, P. W. (1998) *J. Biol. Chem.* 273, 10019–10025.
- Spangler, N. J., Meyers, M. R., Gierke, K. L., Kerby, R. L., Roberts, G. P., and Ludden, P. W. (1998) *J. Biol. Chem.* 273, 4059–4064.
- Anderson, M. E., and Lindahl, P. A. (1994) *Biochemistry* 33, 8702–8711.
- Stephens, P. J., McKenna, M.-C., Ensign, S. A., Bonam, D., and Ludden, P. W. (1989) *J. Biol. Chem.* 264, 16347–16350.
- Ralston, C. Y., Wang, H. X., Ragsdale, S. W., Kumar, M., Spangler, N. J., Ludden, P. W., Gu, W., Jones, R. M., Patil, D. S., and Cramer, S. P. (2000) *J. Am. Chem. Soc.* 122, 10553–10560.
- Russell, W. K., and Lindahl, P. A. (1998) *Biochemistry* 37, 10016–10026.
- Fraser, D. M., and Lindahl, P. A. (1999) *Biochemistry* 38, 15706–15711.
- Heo, J., Staples, C. R., Telser, J., and Ludden, P. W. (1999) *J. Am. Chem. Soc.* 121, 11045–11057.
- Loke, H.-K., Bennett, G., and Lindahl, P. A. (2000) *Proc. Natl. Acad. Sci. U.S.A.* 97, 12530–12535.
- Seravalli, J., Kumar, M., Lu, W. P., and Ragsdale, S. W. (1995) *Biochemistry* 34, 7879–7888.
- Anderson, M. E., and Lindahl, P. A. (1996) *Biochemistry* 35, 8371–8380.
- Staples, C. R., Heo, J., Spangler, N. J., Kerby, R. L., Roberts, G. P., and Ludden, P. W. (1999) *J. Am. Chem. Soc.* 121, 11034–11044.
- Heo, J., Halbleib, C. M., and Ludden, P. W. (2001) *Proc. Natl. Acad. Sci. U.S.A.* 98, 7690–7693.
- Kumar, M., Lu, W.-P., Liu, L., and Ragsdale, S. W. (1993) *J. Am. Chem. Soc.* 115, 11646–11647.
- Maynard, E. L., and Lindahl, P. A. (2001) *Biochemistry* 40, 13262–13267.
- Heo, J., Staples, C. R., and Ludden, P. W. (2001) *Biochemistry* 40, 7604–7611.
- Heo, J., Staples, C. R., Halbleib, C. M., and Ludden, P. W. (2000) *Biochemistry* 39, 7956–7963.
- Xia, J., Hu, Z., Popescu, C., Lindahl, P. A., and Münck, E. (1997) *J. Am. Chem. Soc.* 119, 8301–8312.
- Russell, W. K., Stålhandske, C. M. V., Xia, J., Scott, R. A., and Lindahl, P. A. (1998) *J. Am. Chem. Soc.* 120, 7502–7510.
- Grahame, D. A., and DeMoll, E. (1996) *J. Biol. Chem.* 271, 8352–8358.
- Ragsdale, S. W., Wood, H. G., and Antholine, W. E. (1985) *Proc. Natl. Acad. Sci. U.S.A.* 82, 6811–6814.
- Tucci, G. C., and Holm, R. H. (1995) *J. Am. Chem. Soc.* 117, 6489–6496.
- Fan, C. L., Gorst, C. M., Ragsdale, S. W., and Hoffman, B. M. (1991) *Biochemistry* 30, 431–435.
- Shin, W., Anderson, M. E., and Lindahl, P. A. (1993) *J. Am. Chem. Soc.* 115, 5522–5526.
- Barondeau, D. P., and Lindahl, P. A. (1997) *J. Am. Chem. Soc.* 119, 3959–3970.
- Kumar, M., Qiu, D., Spiro, T. G., and Ragsdale, S. W. (1995) *Science* 270, 628–630.
- Wilson, B. E., and Lindahl, P. A. (1999) *J. Biol. Inorg. Chem.* 4, 742–748.
- Ragsdale, S. W., and Wood, H. G. (1985) *J. Biol. Chem.* 260, 3970–3977.
- Maynard, E. L., and Lindahl, P. A. (1999) *J. Am. Chem. Soc.* 121, 9221–9222.
- Seravalli, J., and Ragsdale, S. W. (2000) *Biochemistry* 39, 1274–1277.
- Maynard, E. L., Sewell, C., and Lindahl, P. A. (2001) *J. Am. Chem. Soc.* 123, 4697–4703.
- Bhaskar, B., DeMoll, E., and Grahame, D. A. (1998) *Biochemistry* 37, 14491–14499.
- Grahame, D. A., and DeMoll, E. (1996) *J. Biol. Chem.* 271, 8352–8358.
- Maupin-Furlow, J. A., and Ferry, J. G. (1996) *J. Bacteriol.* 178, 340–346.